Separation and Purification Technology 232 (2020) 115954

Contents lists available at ScienceDirect

Separation and Purification Technology

journal homepage: www.elsevier.com/locate/seppur

Extraction of phosphorus from metallurgical grade silicon using a combined process of Si-Al-Ca solvent refining and CaO-CaF_2 slag treatment

Chentong Zhang[a,1], Huixian Lai[a,1], Yaohao Zhang[a], Zhilin Sheng[b], Jintang Li[a], Pengfei Xing[c], Xuetao Luo[a,*]

[a] College of Materials, Xiamen University, Xiamen 361005, PR China
[b] School of Material Science and Engineering, Beifang University of Nationalities, Yinchuan 750021, PR China
[c] School of Materials and Metallurgy, Northeastern University, Shenyang 110004, PR China

ARTICLE INFO

Keywords:
Metallurgical grade silicon
Phosphorus removal
Solvent refining
Slag treatment

ABSTRACT

A combined purification process of Si-Al-Ca solvent refining and CaO-CaF_2 slag treatment was investigated with a focus on removing phosphorus (P) from metallurgical-grade Si (MG-Si). The primary precipitates in the slag-treated Si-Al-Ca alloy are $CaAl_2Si_2$ and $CaSi_2$, and these precipitates can be eliminated via leaching with HCl + CH_3COOH and HCl + HF in sequence. Compared to MG-Si, a higher extraction efficiency of P was achieved with Si-Al-Ca alloy after CaO-CaF_2 slag treatment. Influences of alloy composition, slag components, and operation parameter on the P removal efficiency were studied systematically. The optimal dephosphorization efficiency reached 98.6% when the 70%Si-Al-Ca alloy was treated with 20%CaO–80%CaF_2 slag twice. Furthermore, the mechanism of P removal using the combined process was studied. The results indicate that the Si-Al-Ca solvent refining causes the segregation coefficient of P to be lower, thus facilitating its mass transfer in slag treatment. A large amount of P was reduced and then diffused to the slag phase in the slag experiment. Residual P in the slag-treated alloy was trapped by the $CaAl_2Si_2$ phase and was then removed via acid leaching.

1. Introduction

Solar energy is a renewable energy that has the advantages of being clean and widely distributed. It is meaningful to use solar energy to satisfy the thriving demands for energy. Currently, solar grade silicon (SoG-Si), a host material in solar cells, is mainly produced using the improved Siemens process and fluidized bed reactor method [1]. Because both methods are complex and energy-guzzling, exploring an alternative technology for producing SoG-Si is of significant importance. Metallurgical refining is cost-effective, energy-efficient, and regarded as an economic and practical method [2,3].

As featuring different properties of impurities in silicon, various metallurgical purification technologies have been applied to remove different impurities. Traditional processes have included slag treatment [4,5], acid leaching [6,7], vacuum refining [8,9], electron beam melting [10–12], and directional solidification [13,14]. Solvent refining, a promising candidate, has attracted increasing attention because it can promote the removal of impurities in subsequent purification processes, and especially stubborn impurities such as phosphorus (P) and boron (B) can be removed [15,16].

To obtain better removal of impurities, Ma et al. [3,17] proposed an innovative purification technology of slag treatment using Si-Sn alloys. It is noteworthy that a partition ratio of B as high as 200 can be achieved at best, and this is favorable for B removal. A similar technology has also been applied to dephosphorization in the iron and steel industry, in which reducing slag was used because some elements silicon (Si), chromium (Cr), and manganese (Mn) can be readily oxidized before P under oxidizing conditions [18–21]. According to our previous study [22], adding Al and Ca to MG-Si to form the $CaAl_2Si_2$ phase is an effective approach for extracting P from silicon. The activity coefficient of P in the Si-Al-Ca melt increased by dozens of times at low temperature, compared with that in solid silicon. Based on the reported reducing mechanism of P, an increase in the activity coefficient of P in the alloy will increase the distribution ratio of P between the slag and alloy phases, which results in a high removal efficiency of P [18]. In addition, Chen et al. [23] and Shin et al. [18] have used CaO-CaF_2 slag for dephosphorization from Si-Mn(-Fe) and Fe-Ni-Si alloy, respectively. They reported that the CaO-CaF_2 flux exhibited a larger phosphide

* Corresponding author.
E-mail address: xuetao@xmu.edu.cn (X. Luo).
[1] Chentong Zhang and Huixian Lai contributed equally to this work.

https://doi.org/10.1016/j.seppur.2019.115954
Received 28 April 2019; Received in revised form 1 August 2019; Accepted 15 August 2019
Available online 16 August 2019
1383-5866/

Table 1
Major impurity contents of MG-Si and refined MG-Si after treatment via acid leaching with HCl + CH_3COOH and HCl + HF in sequence.

Impurity elements	Impurity concentration (ppmw)					Segregation coefficient [24]
	Source silicon	MG-Si	MG-Si-S	MG-Si-A	MG-Si-AS	
P	35	21	11	5.9	4.5	0.35
Fe	1424	2.6	1.1	1.3	1.3	8.0×10^{-6}
Al	394	28	28	370	390	2.0×10^{-3}
Ca	39	0.84	40	47	30	1.3×10^{-4}–5.2×10^{-4}
Ti	109	0.2	1.9	0.1	0.09	2.0×10^{-6}
Mn	289	0.64	0.22	0.16	0.17	1.3×10^{-5}
Ni	157	0.49	0.52	0.54	0.98	1.4×10^{-5}
Cu	56	0.46	0.15	0.11	0.07	4.0×10^{-4}
V	103	0.1	0.02	0.01	0.02	4.0×10^{-6}
Cr	4.1	0.14	< 0.1	0.13	< 0.1	1.1×10^{-5}
Mg	2.5	0.8	0.66	0.18	0.61	3.0×10^{-6}

"S" denotes MG-Si after slag treatment and "A" denotes it after solvent refining.
"Source silicon" denotes MG-Si lump, which was untreated by leaching.

capacity from 1473 K to 1723 K.

In the present investigation, a combined purification process of Si-Al-Ca solvent refining and CaO-CaF_2 slag treatment was investigated with a focus on P removal from MG-Si. The synergistic effects of alloy composition, slag components, and operation parameter on the P removal efficiency were studied. Subsequently, the dephosphorization mechanism of this method was discussed.

2. Materials and methods

2.1. Materials

To increase the P concentration, SoG-Si (99.9995%) was first mixed with P powder (99.5%) to prepare the SoG-Si-P alloy, which facilitates product characterization. MG-Si lumps (major impurity contents are listed in Table 1), Ca sheets (99.5%), Al powder (99.99%), and the SoG-Si-P sample were used to prepare alloys. The slag consists of reagent-grade CaO and CaF_2. Analytically pure chemicals, including hydrofluoric acid (HF), acetic acid (CH_3COOH), and hydrochloric acid (HCl) were used to prepare all lixiviant.

2.2. Solvent refining

Based on the Si-Al-Ca ternary phase diagram [25], the molar ratio of Ca to Al was kept constant at 1/2 to obtain the maximum $CaAl_2Si_2$ phase for P removal. In addition, the content of silicon in the alloy should exceed 50.9 at.% to obtain the primary silicon crystals during controlled cooling from above the liquidus temperature to the eutectic temperature in the solidification process. Taking these two factors into account, 10 g of samples (composition is listed in Table 2) with Si contents above 70 at.% were prepared in an alumina crucible covered with an alumina lid at 1723 K for 6 h using a horizontal tube furnace under an argon atmosphere. The horizontal tube furnace was then cooled to room temperature at a rate of 5 K/min.

2.3. Slag refining

A binary reducing slag of CaO-CaF_2 was utilized. The prepared Si-Al-Ca(-P) alloy was put into a graphite crucible and then pre-prepared CaO-CaF_2 slag was added. The gross mass of each sample was 15 g, made up of 5 g pretreated alloy and 10 g CaO-CaF_2 slag. Table 2 lists the detailed composition of each sample in the present study. The graphite crucible was placed in the constant temperature zone of a horizontal tube furnace at 1773 K under an argon atmosphere. After holding for 6 h, the temperature of the furnace was decreased to room temperature at a rate of 5 K/min. Finally, the obtained alloy and refined slag were mechanically separated. In addition, MG-Si was directly subjected to the same slag treatment to compare the effects of solvent refining on the P removal via slag treatment.

Table 2
Experimental conditions in the present experiments.

No.	Composition of alloy (at%)				Compositin of slag (at%)		Operation timeof solvent refining	Operation timeof slag treatment
	MG-Si	Al	Ca	SoG-Si-P	CaO	CaF_2		
1	100	0	0	0	0	0	0	0
2	100	0	0	0	20	80	0	1
3	90	6.7	3.3	0	0	0	1	0
4	90	6.7	3.3	0	20	80	1	1
5	90	6.7	3.3	0	5	95	1	1
6	90	6.7	3.3	0	10	90	1	1
7	90	6.7	3.3	0	15	85	1	1
8	90	6.7	3.3	0	25	75	1	1
9	95	3.3	1.7	0	20	80	1	1
10	80	13.3	6.7	0	20	80	1	1
11	70	20	10	0	20	80	1	1
12	70	20	10	0	20	80	1	2
13	0	20	10	70	20	80	1	1

"SoG-Si-P" denotes SoG-Si doped with P.

2.4. Acid leaching

The obtained alloy was ground into powders, and the size was less than 160 μm. To obtain purified Si, two-step sequential acid leaching was carried out under stirring. In the first step, HCl, CH_3COOH and H_2O (1:1:2 by volume) were mixed, and in the second step, HCl, HF, and H_2O (1:1:2 by volume) were mixed. The experimental details of each procedure were that 10 mL of lixiviant was added to 1 g of the alloy sample at 313 K and held for 12 h. The residue solid was separated and rinsed before being dried at the end of each process. To characterize the efficiency of the acid etching, an in situ leaching technology was carried out, the detailed operating parameters were illustrated in our previous study [26].

2.5. Characterization

An electron probe microanalyzer (EPMA) equipped with an energy dispersive spectrometer (EDS) was used to determine the microstructure of samples and the distribution of different impurities. X-ray photoelectron spectroscopy (XPS) with Al Kα radiation was used to analyze the surface chemistry of samples. As a reference to shift the other peaks, the maximum of the C1s peak was set at 284.8 eV for detailed study of the XPS peaks. A Shirley type background line and Gaussian-Lorentzian curves were recorded to deconvolute the peaks.

After acid leaching, glow discharge mass spectrometry (GDMS) was used to measure the impurity concentration of residual silicon.

3. Results and discussion

3.1. Microstructure of Si-Al-Ca alloy after CaO-CaF_2 slag treatment

Most metallic impurities can easily segregate to grain boundaries of Si and further co-precipitate as various intermetallic phases during the solidification process because of their small segregation coefficients (≪1) [27]. Many researchers have reported that the efficiency of removing metallic impurities and the purity of the final silicon are significantly improved by introducing some minor metal components or minor metal compounds to form leachable phases during the solidification process of the alloy [26,28–30]. Therefore, it is meaningful to determine the compositions of the precipitations on the surface of pretreated silicon before the acid leaching process, because various precipitations correspond to different leaching behaviors [26].

It should be noted that the leaching behaviors of MG-Si from different sources are different because they have different precipitations. According to our previous report [26], the main precipitates in the as-received silicon was the Si-Fe phase, and other impurity phases (such as Si-V-Ti, Si-Al-Fe and Si-Ti-Fe phases) were sporadically dispersed in the Si-Fe phase. The P impurity was hardly detected in the precipitates, but it was evenly distributed in the silicon matrix. After alloying with Al and Ca, the Si-Al-Ca phase ($CaAl_2Si_2$) became the primary precipitate in Si and showed a great affinity for P [22].

To improve the removal of P, the silicon was pretreated using a combined purification process of Si-Al-Ca solvent refining and CaO-CaF_2 slag treatment, and the cross-section of ingot is shown in Fig. 1(a). The middle part of the slag-treated alloy area was selected as the sample, and the microstructure of the corresponding slag-treated Si-Al-Ca alloy and the EDS analysis of the primary precipitation phases are shown in Fig. 1(b). It is obvious that the Si-Al-Ca and Si-Ca phases were the main precipitates, and some minor precipitations such as Si-Ca-Fe-Al and Si-Fe-Ti-Mn were also found in the Si-Al-Ca phase. According to the atomic ratio of Si, Al, and Ca, it can be speculated that the main precipitates are $CaAl_2Si_2$ and $CaSi_2$.

To investigate the distribution of P between the silicon matrix and primary precipitations, a master alloy with high P concentration (Si-Al-Ca-P alloy) was used as feedstock in the slag treatment trial. The EPMA mapping analysis of the Si-Al-Ca-P alloy after 15 at.% CaO-CaF_2 slag treatment is shown in Fig. 2. Concentrated P was only found in the $CaAl_2Si_2$ phase and no P was fund in the $CaSi_2$ phase. Similar results were also reported by several researches [6,26,31–34]. However, a contrary result was reported by Shimpo et al. [35], in which P was inclined to dissolve in the $CaSi_2$ phase when Si was alloyed with Ca. According to our previous study [22], the activity coefficient of P impurity in the Si-Al-Ca melt is lower than that in solid silicon phase during the solidification process, which indicates that P impurity tended to be trapped in the $CaAl_2Si_2$ phase. If the phase with a high content of P can be leached out by the lixiviant, a high efficiency in removing P impurity can be achieved.

3.2. Separation of Si from the slag-treated Si-Al-Ca alloy

To test the acid sensitivity of the precipitations in the refined silicon, the in situ etching technique was used [4,26]. The polished surface of the sample was immersed in the etchant and the corresponding results are presented in Fig. 3. First, the primary phases involving $CaAl_2Si_2$ and $CaSi_2$ phase (grey) but most of minor precipitations (grey white) can be dissolved in the mixture of HCl + CH_3COOH after etching for 2 h, and this is in agreement with previous reports [4,26,28]. However, all residual precipitations were dissolved after further etching with the mixture of HCl + HF. There are no insoluble phases in the surface of the silicon matrix. Therefore, the precipitation phases in the slag-treated Si-Al-Ca alloy can be readily separated from the alloy after leaching with HCl + CH_3COOH and HCl + HF in sequence. It is expected that a highly pure of silicon with low P concentration can be obtained.

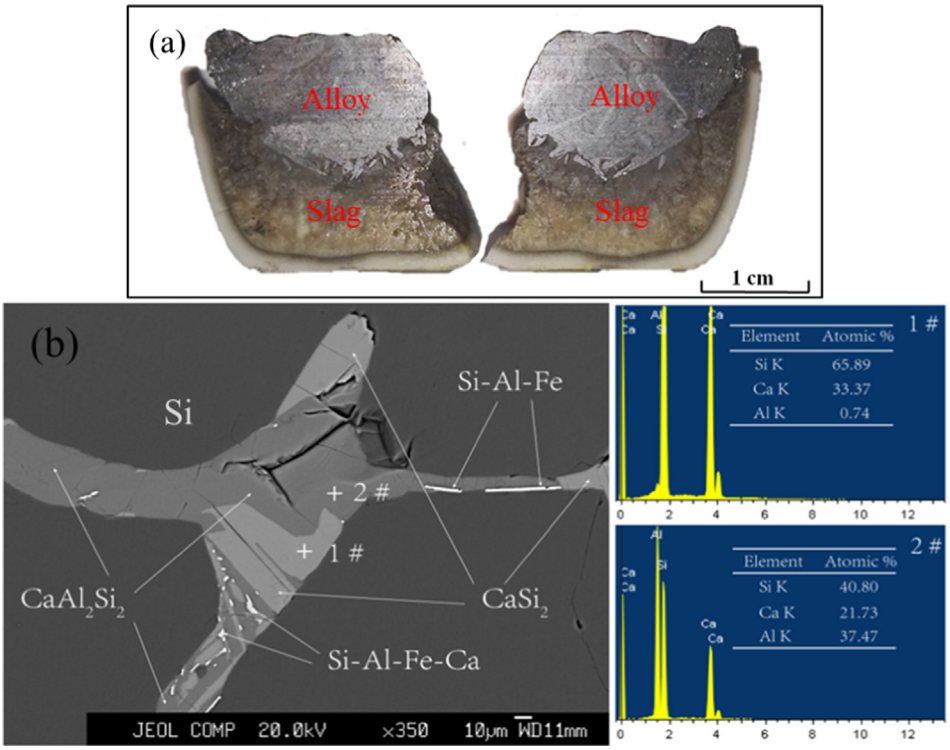

Fig. 1. (a) Cross-section of ingot after the combined process of Si-Al-Ca solvent refining and CaO-CaF_2 slag treatment; (b) microstructure of the sample and the corresponding EDS analysis.

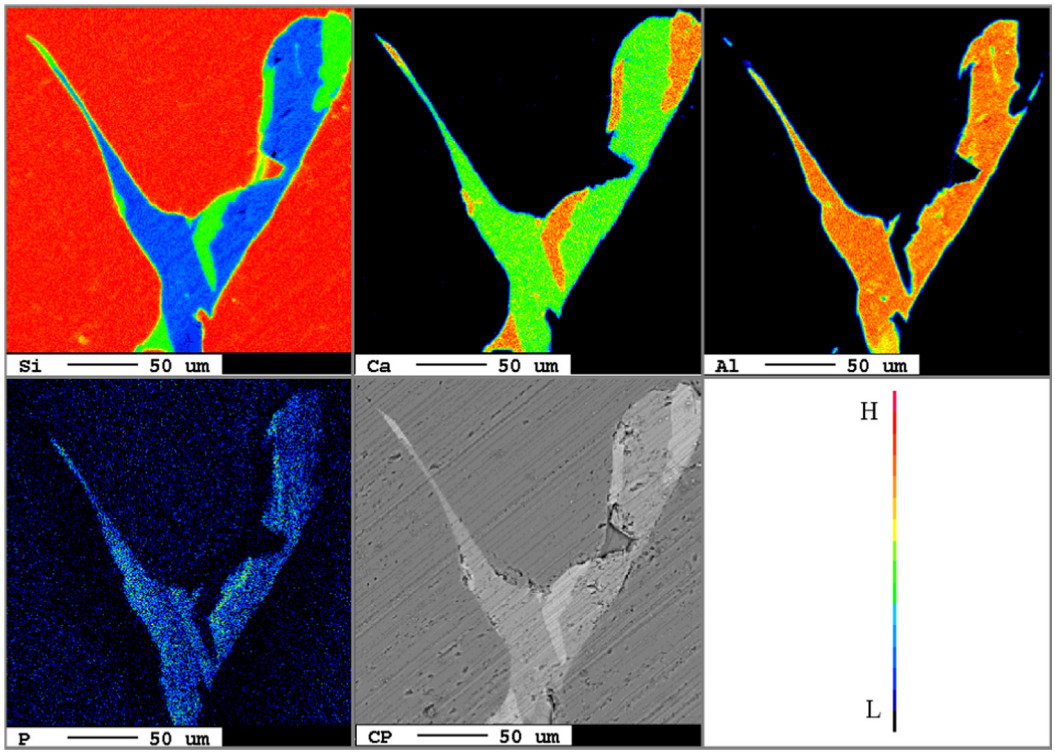

Fig. 2. EPMA mapping analysis of the Si-Al-Ca-P alloy after 15 at.% CaO-CaF_2 slag treatment.

3.3. Comparison of different pretreatment technologies

Acid leaching, slag treatment and solvent refining were applied alone or jointly to compare the effects of different pretreatment techniques for MG-Si on impurity removal efficiency, and the experimental results are summarized in Table 1. With the exception of P, the concentration of most metallic impurities in MG-Si, including Cu, Ti, Mn, Ni, Cr and V, is significantly decreased by direct acid leaching. The results indicate that leaching MG-Si without any pretreatment can efficiently remove metallic impurities but cannot effectively remove P impurity. A similar phenomenon has also been reported by several researchers [4,29,36]. According to our previous research, P impurity cannot be removed effectively because of its uniform distribution in the silicon matrix [26]. After slag treatment, the concentration of P in the resulting silicon decreases from 35 ppmw to 11 ppmw by acid leaching, which less than 21 ppmw achieved directly. It follows that slag treatment using CaO-CaF_2 slag is conducive to removing P impurity from MG-Si. However, the concentration of Ca increases because of the use of Ca-containing slag. Nevertheless, the concentration of Ca in refined silicon can be reduced effectively by the subsequent purification procedures, such as vacuum [14,37] and directional solidification [24]. After solvent refining, the concentration of all impurities, including P, were significantly decreased. Compared to the silicon obtained via slag treatment, a lower concentration of P can be achieved via solvent refining. After pretreating MG-Si through a combined purification process of solvent refining and slag treatment, the lowest concentration of P in the resulting silicon was as low as 4.5 ppmw. This was because the activity coefficient of P in the Si-Al-Ca alloy was several times higher than that of P in solid silicon, and this favored to an increased distribution ratio of P between the slag and metal phases [18,22,23]. Similar findings were also reported by Ma et al. [17], who proposed that when the activity coefficient of B was increased significantly with an increase in Sn content in the Si-Sn alloy, the partition ratio of B also increased during the slag treatment. The value of the partition ratio was as high as 200 when the Si-82.4 at.% Sn alloy was used. Thus, the combined purification process of Si-Al-Ca solvent refining and CaO-CaF_2 slag treatment is most conducive for removing P impurity via acid leaching.

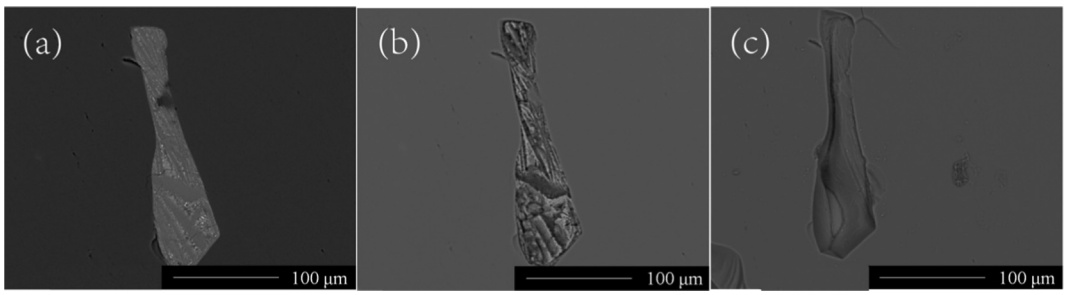

Fig. 3. Micro-structural evolution of MG-Si treated using a combined purification process of Si-Al-Ca solvent refining and CaO-CaF_2 slag treatment after etching with different lixiviants: (a) original microstructure, (b) after exposure to 2 M HCl + CH_3COOH for 2 h, and (c) after exposure to 2 M HCl + HF for 2 h in sequence, Temperature: 298 K.

3.4. Removal of P impurity

3.4.1. Effects of slag composition

The CaO content of CaO-CaF_2 slag were changed to study the influence of slag composition on dephosphorization efficiency (De-P efficiency) of the combined process. Here, the De-P efficiency (η_{De-P}) is calculated using Eq. (1):

$$\eta_{De-P} = \frac{\omega[P]^o - \omega[P]^f}{\omega[P]^o} \times 100\% \quad (1)$$

where $\omega[P]^o$ and $\omega[P]^f$ refer to the concentration of P in samples before and after the combined process, respectively. According to the removal mechanism of P under highly reducing conditions, it is considered that P impurity is dissolved into the flux in the form of phosphide ions as follows [18,23]:

$$[P]_{Si-Al-Ca} + \frac{3}{2}(O^{2-}) = (P^{3-}) + \frac{3}{4}O_2(g) \quad (2)$$

$$K = \frac{a_{P^{3-}} \cdot P_{O_2}^{0.75}}{a_P \cdot a_{O^{2-}}^{1.5}} = \frac{f_{P^{3-}} \cdot X_{P^{3-}}}{f_P \cdot X_P} \cdot \frac{P_{O_2}^{0.75}}{a_{O_2}^{1.5}} \quad (3)$$

where $a_{P^{3-}}$ and $f_{P^{3-}}$ represent the activity and activity coefficient, respectively, of the phosphide in the slag phase; a_P and f_P represent the activity and activity coefficient, respectively, of P in the Si-Al-Ca alloy phase; $a_{O^{2-}}$ is the activity of free oxygen, and P_{O_2} is the partial pressure of oxygen. The phosphide capacity ($C_{P^{3-}}$) of the slag treatment can be defined according to the following equation:

$$C_{P^{3-}} = \frac{K \cdot a_{O^{2-}}^{1.5}}{f_{P^{3-}}} = L_P \cdot \frac{P_{O_2}^{0.75}}{f_P} \quad (4)$$

$$L_P = (X_{P^{3-}})/[X_P] \quad (5)$$

where L_P represents the distribution ratio of P between the slag and Si-Al-Ca alloy. The relationship between CaO content and De-P efficiency obtained in this experiment is shown in Fig. 4. A significant increase in De-P efficiency appears with an increase in CaO content, up to about 20 at.%, and this is mainly because the concentration of O^{2-} increases with an increase in CaO content, which makes the chemical equilibrium of Eq. (2) shift to the right. A similar phenomenon was also reported by Shin and Park [18]. According to the CaO-CaF_2 binary phase diagram [20], the flux of solid lime is saturated when the CaO contents in CaO-CaF_2 slag is greater than about 20 wt%, indicating that the activity of free O^{2-} is approximately constant [38]. Therefore, the De-P efficiency remains constant at this stage because the O^{2-} activity becomes constant. Nassaralla et al. [20] also reported that in Fe-C-P alloys.

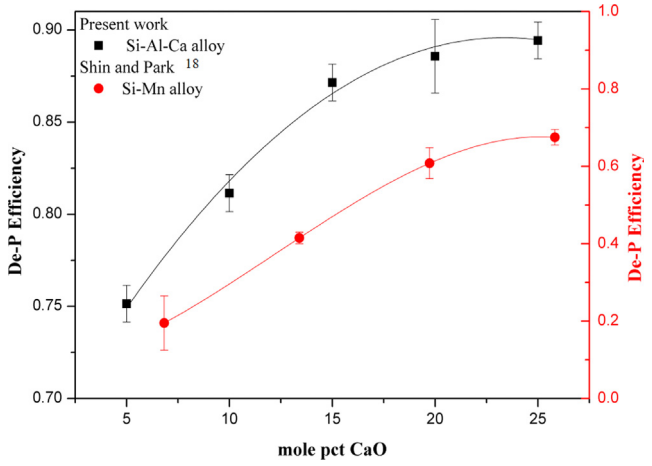

Fig. 4. Relationship between CaO content and De-P efficiency.

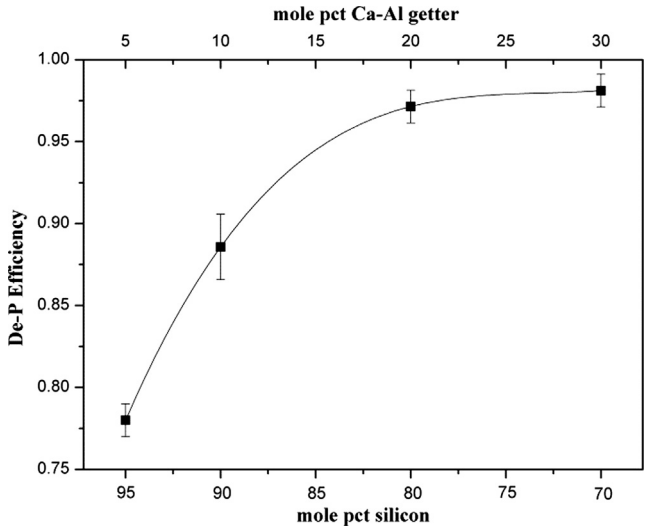

Fig. 5. Relationship between Si content and De-P efficiency.

3.4.2. Effects of alloy composition

Si content was varied over the range of 70–95 at.% to investigate the effects of alloy composition on De-P efficiency of the combined process. When the Si-Al-Ca alloy was treated with 20 at.% CaO-CaF_2, the relationship between Si content and De-P efficiency was obtained in this experiment and is presented in Fig. 5. With a decrease in Si content, the De-P efficiency increased, and the highest removal efficiency of P was 98.1%. When more solvents were used, there was increased dissolution of P impurity in the Si-Al-Ca phase. Thus, reducing the Si content in Si-Al-Ca alloys is favorable for obtaining higher De-P efficiency. However, considering the cost of solvent refining, the alloy composition with 70 at.% Si-20 at.% Al-Ca was chosen.

3.4.3. Effects of operation time of slag treatment

A continuous slag refining was performed at 1773 K to observe the influence of the operation time of slag treatment on P removal. The experimental results after the first and second runs are presented in Table 3. The concentration of P in the refined silicon decreased from 35 ppmw to 1 ppmw with a removal efficiency of 97.1% after the first run. After the second slag refining, the P concentration was further decreased to 0.5 ppmw with a removal efficiency of 98.6%.

3.5. Mechanism of P removal from Si-Al-Ca alloys via CaO-CaF_2 slag treatment

To investigate the mechanism of P removal from Si-Al-Ca alloys via CaO-CaF_2 slag treatment, XPS analysis was applied to determine the chemical state of P in the samples. In this case, the SoG-Si-doped P was used as feedstock to prevent the influences of other impurities and to facilitate product characterization. The results of XPS analysis experiments are shown in Fig. 6. As seen in Fig. 6(a), after the doping experiment, the P 2p line of SoG-Si-P can be divided into two doublets. The $2p_{3/2}$ peak positions of these doublets are located at 134.6 eV and 129.1 eV. The peak of P 2p at 134.6 eV is attributed to oxidized P [39]. Compared to the binding energy of elemental P (130 eV), the second peak presented at 129.1 eV was negatively shifted about 0.9 eV, and this indicates that P accepts a partial electron from silicon and accordingly forms SiP [39–41].

To analyze the state of P in Si-Al-Ca alloys, SoG-Si-P was used as the source silicon to prepare Si-Al-Ca-P alloys. High resolution of XPS spectra for P is presented in Fig. 6(b). As seen in Fig. 6(b), the P 2p spectra of Si-Al-Ca-P was successfully fitted to one peak with the main peak of P $2p_{3/2}$ (132.7 eV). This indicates that only one type of P compounds was presented in the structure. The binding energy of the

Table 3
Experimental conditions and results of a consecutive slag treatment at 1773 K.

Refining times	Initial alloy	Initial slag	P content in resulting silicon after run	P removal (%)
First run	70 at.% Si–20 at.% Al-Ca	20 at.% CaO-CaF_2	1	97.1
Second run	The alloy after first run	20 at.% CaO-CaF_2	0.5	98.6

peak can be assigned to oxidized P [39,40,42]. According to the above result, there are two possibilities for explaining this phenomenon. The first possibility is that the oxidized P was formed during melting Si-Al-Ca-P alloy. And the other is that the P-containing product was oxidized after the alloying. The former is almost impossible as Si-Al-Ca-P alloy was melted and cooled down to room temperature under argon atmosphere. Therefore, the latter is more likely to happen. A similar phenomenon was also observed in the Si-Al-Ca-P alloy after slag treatment, as shown in Fig. 6(c). In this case, slag treatment was performed under Argon atmosphere. Therefore, we can surmise that that the P-containing product was oxidized after alloying. However, a lower concentration of phosphide in the alloy can be achieved after slag treatment because under highly reducing conditions, it is expected that P dissolves into the flux as phosphide as follows [18,19]:

$$2(CaO) + [Si] = (SiO_2) + 2[Ca] \quad (6)$$

$$3[Ca] + 2[P] = (Ca_3P_2) \quad (7)$$

Because Ca_3P_2 is very active when it is in contact with moisture, the hazardous phosphine gas will evolve according to the following reactions:

$$Ca_3P_2(s) + 3H_2O(g) = 3CaO(s) + 2PH_3(g) \quad (8)$$

$$Ca_3P_2(s) + 6H_2O(g) = 3Ca(OH)_2(s) + 2PH_3(g) \quad (9)$$

The similar phenomenon was also reported by several research teams [18,19,23]. Furthermore, $Ca_3(PO_4)_2$ will form when Ca_3P_2 contact with the oxygen as follow:

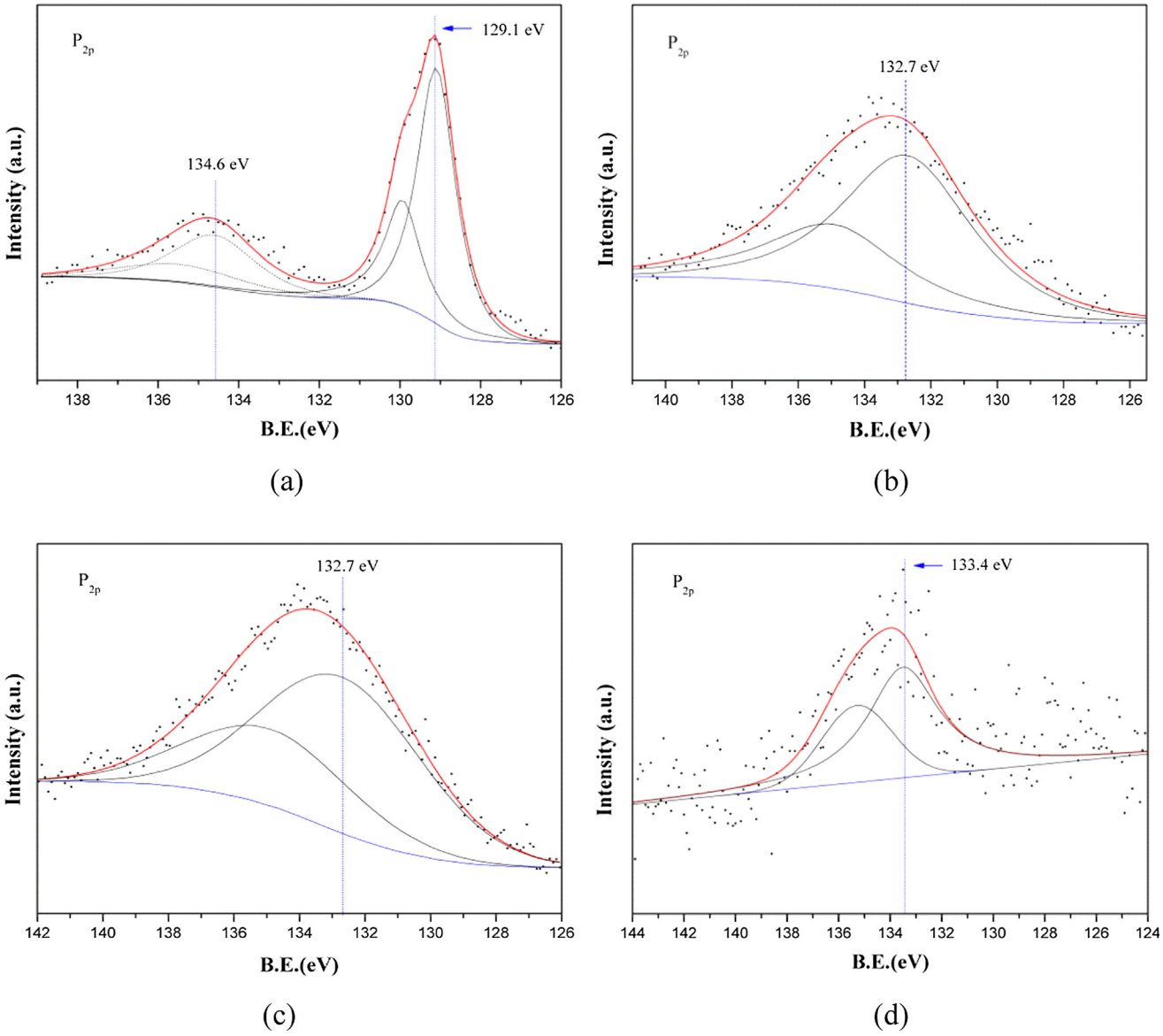

Fig. 6. High resolution XPS spectra of (a) SOG-Si-P, (b) Si-Al-Ca-P alloy before and (c) after slag treatment, (d) as well as the resulting slag.

$$Ca_3P_2(s) + 4O_2(g) = Ca_3(PO_4)_2 \quad (10)$$

According to the results calculated by using HCS chemistry 6 software, the change in standard Gibbs free energy of these reactions has significantly negative values at room temperature, which indicates that it is possible to create PH_3 andPO_4^{3-} at room temperature. Therefore, the P_{2p} spectra of Si-Al-Ca-P alloy before and after slag treatment are both regarded as PO_4^{3-}. As shown in Fig. 6(d), the P $2p_{3/2}$ binding energy of the resulting slag is about 133.4 eV, which is higher than that of refined Si-Al-Ca alloy. This indicates that the oxidation state of P in the resulting slag is higher than that in the Si-Al-Ca alloy to some extent. Thus, the P in the resulting slag may exist in an octahedral environment rather than as PO_4^{3-} in a tetrahedral environment [42].

In our point of view, it can be speculated that the two main approaches were combined to remove P impurity from the Si-Al-Ca alloy in the combined purification process. First, P-containing compounds were formed at the interface between the slag and Si-Al-Ca alloy, and these then diffused into the slag during slag treatment. Second, most of residual P impurity still dissolved in the $CaAl_2Si_2$ phase, and this was removed with the dissolution of precipitations after further etching.

4. Conclusions

In this paper, a combined process of Si-Al-Ca solvent refining and CaO-CaF_2 slag treatment was applied to purify metallurgical grade silicon (MG-Si). Apart from the $CaAl_2Si_2$ phase, $CaSi_2$ was also found in MG-Si after pretreatment via solvent refining and slag treatment, whereas no P was detected in this phase. All of these phases can be dissolved after leaching with HCl + CH_3COOH and HCl + HF in sequence. Compared to the resulting silicon obtained by slag treatment pretreatment, a lower concentration of P could be achieved by solvent refining pretreatment. However, after pretreating MG-Si by a combined process of solvent refining and slag treatment, the obtained resulting silicon showed the lowest concentration of P. Therefore, the Si-Al-Ca solvent refining technology can improve the P removal capacity of the CaO-CaF_2 slag treatment. The dephosphorization efficiency increased with an increase in the CaO content up to the CaO saturation point in the CaO-CaF_2 flux in 1773 K. Decreasing the silicon content in the alloy can increase the P removal efficiency and the P concentration as low as 0.5 ppmw was achieved when 70%Si-Al-Ca alloy was twice treated with 20%CaO-80%CaF_2 slag. XPS was conducted to detect the surface chemical state of the as-prepared samples and found that P in the silicon was first reduced in the present experiment and was oxidized when it was in contact with air. To some extent, the oxidation state of P in the resulting slag was higher than that in the refined Si-Al-Ca alloy.

Acknowledgement

This work was supported by the National Natural Science Foundation of China (No. 51334004).

References

[1] J.J. Wu, D. Yang, M. Rekinger, M. Xu, Boron removal from silicon using secondary refining techniques by metallurgical method, Sep. Purif. Rev. (2018) 1–21.
[2] M.D. Johnston, L.T. Khajavi, M. Li, S. Sokhanvaran, M. Barati, High-temperature refining of metallurgical-grade silicon: a review, JOM 64 (2012) 935–945.
[3] X.D. Ma, T. Yoshikawa, K. Morita, Purification of metallurgical grade Si combining Si-Sn solvent refining with slag treatment, Sep. Purif. Technol. 125 (2014) 264–268.
[4] M. Fang, C.H. Lu, L.Q. Huang, H.X. Lai, J. Chen, J.T. Li, W.H. Ma, P.F. Xing, X.T. Luo, Effect of calcium-based slag treatment on hydrometallurgical purification of metallurgical-grade silicon, Ind. Eng. Chem. Res. 53 (2014) 972–979.
[5] Z. Ding, W.H. Ma, K.X. Wei, X.X. Wu, Y. Zhou, K.Q. Xie, Boron removal from metallurgical-grade Silicon using lithium containing slag, J. Non-Cryst. Solids 358 (2012) 2708–2712.
[6] H.X. Lai, L.Q. Huang, H.P. Xiong, C.H. Gan, P.F. Xing, J.T. Li, X.T. Luo, Hydrometallurgical purification of metallurgical grade silicon with hydrogen peroxide in hydrofluoric acid, Ind. Eng. Chem. Res. 56 (2017) 311–318.
[7] S.K. Sahu, E. Asselin, Effect of oxidizing agents on the hydrometallurgical purification of metallurgical grade silicon, Hydrometallurgy 121 (2012) 120–125.
[8] S.S. Zheng, T.A. Engh, M. Tangstad, X.T. Luo, Separation of phosphorus from silicon by induction vacuum refining, Sep. Purif. Technol. 82 (2011) 128–137.
[9] K. Suzuki, K. Sakaguchi, T. Nakagiri, N. Sano, Gaseous removal of phosphorus and boron from molten silicon, J. Non-Cryst. Solids 54 (1990) 161–167.
[10] S. Shi, W. Dong, X. Peng, D.C. Jiang, Y. Tan, Evaporation and removal mechanism of phosphorus from the surface of silicon melt during electron beam melting, Appl. Surf. Sci. 266 (2013) 344–349.
[11] J.C.S. Pires, J. Otubo, A.F.B. Braga, P.R. Mei, The purification of metallurgical grade silicon by electron beam melting, J. Mater. Process. Technol. 169 (2005) 16–20.
[12] Y. Tan, X.L. Guo, S. Shi, W. Dong, D.C. Jiang, Study on the removal process of phosphorus from silicon by electron beam melting, Vacuum 93 (2013) 65–70.
[13] M.A. Martorano, J.B.F. Neto, T.S. Oliveira, T.O. Tsubaki, Refining of metallurgical silicon by directional solidification, Mater. Sci. Eng., B 176 (2011) 217–226.
[14] Y. Tan, S.Q. Ren, S. Shi, S.T. Wen, S.T. Jiang, W. Dong, M. Ji, S.H. Sun, Removal of aluminum and calcium in multicrystalline silicon by vacuum induction melting and directional solidification, Vacuum 99 (2014) 272–276.
[15] L. Lei, Z.H. Ma, J.J. Wu, S.Y. Li, K. Morita, Impurity phases and their removal in Si purification with AleSi alloy using transition metals as additives, J. Alloys Compd. 734 (2018) 250–257.
[16] L.Q. Huang, A. Danaei, S. Thomas, P.F. Xing, J.T. Li, X.T. Luo, M. Barati, Solvent extraction of phosphorus from Si-Cu refining system with calcium addition, Sep. Purif. Technol. 204 (2018) 205–212.
[17] X.D. Ma, T. Yoshikawa, K. Morita, Removal of boron from silicon-tin solvent by slag treatment, Metall. Mater. Trans. B 44 (2013) 1–6.
[18] J.H. Shin, J.H. Park, Thermodynamics of reducing refining of phosphorus from Si-Mn alloy using CaO-CaF_2 slag, Metall. Mater. Trans. B 43 (2012) 1243–1246.
[19] J.H. Shin, J.H. Park, Effect of atmosphere and slag composition on the evolution of PH_3 gas during cooling of reducing dephosphorization slags, ISIJ Int. 53 (2013) 385–390.
[20] C. Nassaralla, R.J. Fruehan, D.J. Min, A thermodynamic study of dephosphorization using BaO-BaF_2, CaO-CaF_2, and BaO-CaO-CaF_2 systems, Metall. Mater. Trans. B 22 (1991) 33–38.
[21] C. Nassaralla, R.J. Fruehan, Phosphate capacity of CaO-AI_2O_3 slags containing CaF_2, BaO, Li_2O, or Na_2O, Metall. Mater. Trans. B 23 (1992) 117–123.
[22] H.X. Lai, Z.L. Sheng, J.T. Li, P.F. Xing, X.T. Luo, Enhanced separation of phosphorus from metallurgical grade silicon by $CaAl_2Si_2$ phase reconstruction, Sep. Purif. Technol. 191 (2018) 257–265.
[23] P.X. Chen, G.H. Zhang, S.J. Chu, Study on reaction mechanism of reducing dephosphorization of Fe-Ni-Si Melt by CaO-CaF_2 slag, Metall. Mater. Trans. B 47 (2016) 16–18.
[24] F.A. Trumbore, Citation classic-solid solubilities of impurity elements in germanium and silicon, Bell Syst. Tech. J. 39 (1960) 205–233.
[25] J.C. Anglezio, C. Servant, I. Ansara, Contribution to the experimental and thermodynamic assessment of the Al-Ca-Fe-Si system. Al-Ca-Fe, Al-Ca-Si, Al-Fe-Si and Ca-Fe-Si systems, CALPHAD: Comput. Coupl. Phase Diagrams Thermochem. 18 (1994) 273–309.
[26] H.X. Lai, L.Q. Huang, C.H. Lu, M. Fang, W.H. Ma, P.F. Xing, J.T. Li, X.T. Luo, Leaching behavior of impurities in Ca-alloyed metallurgical grade silicon, Hydrometallurgy 156 (2015) 173–181.
[27] C.D. Thubmond, M. Kowalchik, Germanium and silicon liquidus curves, Bell Syst. Tech. J. 39 (2013) 169–204.
[28] F. Margarido, M.O. Figueiredo, A.M. Queiroz, J.P. Martins, Acid leaching of alloys within the quaternary system Fe-Si-Ca-Al, Ind. Eng. Chem. Res. 36 (1997) 5291–5295.
[29] F.L. He, S.S. Zheng, C. Chen, The effect of calcium oxide addition on the removal of metal impurities from metallurgical-grade silicon by acid leaching, Metall. Mater. Trans. B 43 (2012) 1011–1018.
[30] Y.V. Meteleva-Fischer, Y. Yang, R. Boom, B. Kraaijveld, H. Kuntzel, Microstructure of metallurgical grade silicon during alloying refining with calcium, Intermetallics 25 (2012) 9–17.
[31] J.C. Anglezio, C. Servant, F. Dubrous, Characterization of metallurgical grade silicon, J. Mater. Res. 5 (1990) 1894–1899.
[32] L.Y. Sun, Z. Wang, H. Chen, D. Wang, G.Y. Qian, Removal of phosphorus in silicon by the formation of $CaAl_2Si_2$ phase at the solidification interface, Metall. Mater. Trans. B 48 (2016) 420–428.
[33] T.H. Ludwig, E.S. Dæhlen, P.L. Schaffer, L. Arnberg, The effect of Ca and P interaction on the Al-Si eutectic in a hypoeutectic Al-Si alloy, J. Alloys Compd. 586 (2014) 180–190.
[34] Y.V. Meteleva-Fischer, Y.X. Yang, R. Boom, B. Kraaijveld, H. Kuntzel, Slag treatment followed by acid leaching as a route to solar-grade silicon, JOM 64 (2012) 957–967.
[35] T. Shimpo, T. Yoshikawa, K. Morita, Thermodynamic study of the effect of calcium on removal of phosphorus from silicon by acid leaching treatment, Metall. Mater. Trans. B 35 (2004) 277–284.
[36] H.X. Lai, L.Q. Huang, C.H. Gan, P.F. Xing, J.T. Li, X.T. Luo, Enhanced acid leaching of metallurgical grade silicon in hydrofluoric acid containing hydrogen peroxide as oxidizing agent, Hydrometallurgy 164 (2016) 103–110.
[37] J. Safarian, M. Tangstad, Vacuum refining of molten silicon, Metall. Mater. Trans. B 43 (2012) 1427–1445.
[38] W.G. Seo, D.H. Zhou, F. Tsukihashi, Calculation of thermodynamic properties and phase diagrams for the CaO-CaF_2, BaO-CaO and BaO-CaF_2 systems by molecular dynamics simulation, Mater. Trans. 46 (2005) 643–650.
[39] J.F. Moulder, W.F. Stickle, P.E. Sobol, K.D. Bomben, Handbook of X-ray Photoelectron Spectroscopy, Physical Electronics, Inc., 1992, pp. 58–59.
[40] H. Li, H.X. Li, W.L. Dai, Z.G. Fang, Z.F. Deng, XPS studies on surface electronic characteristics of Ni-B and Ni-P amorphous alloy and its correlation to their catalytic properties, Appl. Surf. Sci. 152 (1999) 25–34.
[41] P.A. Bertrand, XPS study of chemically etched GaAs and lnP, J. Vac. Sci. Technol. 1 (1981) 28–33.
[42] R.Y. Zheng, L. Lin, J.L. Xie, Y.X. Zhu, Y.C. Xi, State of doped phosphorus and its influence on the physicochemical and photocatalytic properties of P-doped titania, J. Phys. Chem. C 112 (2008) 15502–15509.